Scottish Universities Environmental Research Centre

Luminescence Profile Measurements on Samples from Vietnam Submitted by P. Carling

March 2018

A.J. Cresswell[1], D.C.W. Sanderson[1], P.A. Carling[2]

[1] SUERC, East Kilbride, Glasgow
[2] Geography and Environment, University of Southampton

East Kilbride Glasgow G75 0QF Telephone: 01355 223332 Fax: 01355 229898

Summary

Luminescence measurements have been conducted on small samples from a stratigraphic horizon in Vietnam overlaying a regionally extensive gravel layer containing tektites and shocked quartz that are evidence for a meteorite impact dated to approximately 700 ka. The lower part of this stratigraphic horizon contains coarser grains and smashed granules which may also be associated with the impact event. Profiling measurements of the same sedimentary feature in Thailand showed an inverted luminescence profile. The measurements conducted here show that these materials had been very well bleached prior to deposition, with bright rapidly depleting OSL signals from quartz grains. These samples do not reproduce the inverted sequence observed in Thailand. The OSL measurements suggest three distinct zones within the sedimentary sequence; the youngest 6-7 samples showing a steady increase in stored dose estimates, the middle 7-8 samples show approximately constant dose estimates, with a discontinuity in dose estimate above the oldest 7-8 samples which also show a higher OSL depletion rate and IRSL:OSL ratio. It is suggested that the data represent a history of rapid sedimentation depositing the lower zone, followed by an erosional event removing the upper part of this sequence, before a second period of rapid sedimentation with material potentially from a different source, and finally a more recent period of lower sedimentation rate. These samples appear to be very suitable for quantitative dating with sufficient material for dose rate determination in some instances, and could be considered for establishing a chronology for this stratigraphic sequence. Quantitative SAR OSL analysis has been conducted on three samples, one from each of the three zones, where control samples had been collected providing sufficient material for dose rate calculation. There are differences between the three samples in both dose rate (upper sample with the lowest dose rate and the lower sample the highest) and luminescence sensitivity (with the lowest sample being less sensitive), suggestive of differences in the source materials for each of the three zones. The SAR ages for the upper two samples are inverted and significantly different from the profiling apparent ages (16.0 ± 2.3 ka for the upper and 5.4 ± 0.7 ka for the middle sample). The lowest sample, just above the gravel layer containing shocked quartz and tektites, has an equivalent dose distribution with a broad peak corresponding to an age of 14 ± 2 ka, with several aliquots with equivalent doses that correspond to ages significantly in excess of 50 ka. The 14 ± 2 ka age is consistent with previous OSL ages for the corresponding sedimentary layer in Thailand (8 and 19 ka), which is significantly younger than the impact date and suggest that these layers are not associated with the impact. However, the significantly older ages for some samples may suggest an earlier deposition with subsequent disturbance introducing the younger material. Alternative quartz analysis methods would be needed to extend the range of measurement to explore the age of these older components.

Contents

List of figures

List of tables

1. Introduction

Investigations have been undertaken of a regionally extensive feature covering parts of Thailand and Vietnam. This consists of apparently near homogenous deposits of fine sand, often several meters thick, overlaying an extensive gravel layer. The gravel contains abundant tektites and shocked quartz, clearly identified as a meteorite impact layer, with the tektites securely dated to c. 700,000 BP. The lower 10-20 cm of the sand layer is coarser than the upper layers, and contains abundant smashed granules which may relate to the impact, potentially atmospheric fallout deposit.

Sampling and luminescence profiling of the sedimentary layers in Thailand had been collected in 2015 (Carling pers.comm.), showing inverted profiles (Figure 1.1) with larger OSL counts at the top of the profile, especially for the Krahad profile. Possible explanations for this inversion include changes in sensitivity, changes in dosimetry or residual signals or reworking of sediments. The IRSL counts from these samples were much smaller. Luminescence dates for the lower (granule) layers in these profiles yielded ages of 8,000 and 19,000 BP. Thus if the dates are correct the granule layer cannot be related to the impact, and its origin becomes difficult to explain.

Previous studies of this feature elsewhere in the region (Sanderson et.al. 2001) have reported a range of models proposed to explain the characteristics and origin of this layer, including Late Pleistocene or Holocene aeolian deposits, lacustrine, marine or fluvial deposits, or development of the layer from the emplacement and subsequent weathering of termite mounds. This study in Khon Kaen region of NE Thailand measured luminescence from six samples in the top 2m of this feature, with results that suggested a largely aeolian deposit, though some bioturbation could have contributed to the luminescence characteristics, with ages of ~35ka determined for the lowest samples.

To further investigate this, two further profiles from the same stratigraphic horizon have been collected from Vietnam, with one of these profiles submitted for luminescence profile analysis. Three control samples from the same section were collected, and exposed to intense daylight for 2h.

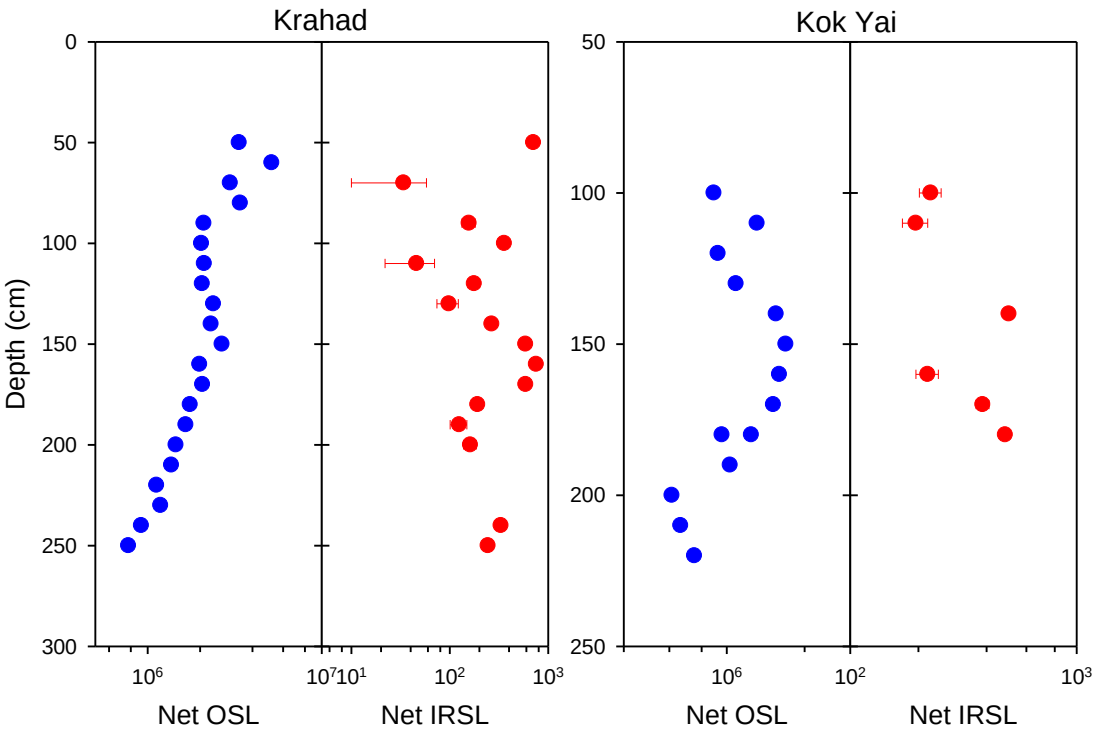

Figure 1.1: Portable instrument profiles for two sites measured in Thailand in 2015, showing inverted OSL profiles, especially for the Krahad site.

2. Methods

Each sample was given a laboratory (SUTL) reference code upon receipt at SUERC, as summarised in Table 2.1. Samples were numbered from 1 (10 cm above the gravel layer) upwards and collected at 10 cm intervals, and have been assigned nominal depths shown in Table 2.1. The SUTL2969 samples were 20-25 g, with 40-50 g for the control samples.

Table 2.1: Summary of samples and SUERC laboratory reference codes

Profile position	Nominal depth (cm)	Sample SUERC code	Control SUERC code
1	210	SUTL2969/1	SUTL2970A
2	200	SUTL2969/2	
3	190	SUTL2969/3	
4	180	SUTL2969/4	
5	170	SUTL2969/5	
6	160	SUTL2969/6	
7	150	SUTL2969/7	
8	140	SUTL2969/8	
9	130	SUTL2969/9	SUTL2970B
10	120	SUTL2969/10	
11	110	SUTL2969/11	
12	100	SUTL2969/12	
13	90	SUTL2969/13	
14	80	SUTL2969/14	
15	70	SUTL2969/15	
16	60	SUTL2969/16	
17	50	SUTL2969/17	SUTL2970C
18	40	SUTL2969/18	
19	30	SUTL2969/19	
20	20	SUTL2969/20	
21	10	SUTL2969/21	

2.1. Portable OSL measurements

All samples were first appraised using the SUERC portable OSL reader, following an interleaved sequence of system dark count (background), infra-red stimulated luminescence (IRSL) and OSL, similar to that described by Sanderson and Murphy (2010). This method allows for the calculation of IRSL and OSL net signal intensities, depletion indices and IRSL:OSL ratios, which are then used to generate luminescence-depth profiles.

2.2. Laboratory Profile Measurements

2.2.1. Sample preparation

Simple calibrated laboratory luminescence screening measurements (cf. Burbidge et al., 2007; Sanderson et al., 2001; Sanderson et al., 2007) were undertaken on polymineral and quartz fractions to provide the first preliminary assessment of sensitivities and stored dose estimates throughout the sampled profile.

All sample handling and preparation was conducted under safelight conditions in the SUERC luminescence dating laboratories. A small portion of each sample (~2 g) was wet sieved to extract the 90-250 µm grain size fraction. This was subjected to an acid treatment of 1M HCl for 10 minutes, 15% HF for 15 mins and 1M HCl for 10 mins, with the sample washed thoroughly with deionised water between each treatment. Approximately half of the material was retained, washed in acetone to displace water and dried as a polymineral sample. The remaining material was subjected to a further acid treatment of 40% HF for 40 mins and 1M HCl for 10 mins, with the sample washed thoroughly with deionised water between each treatment. This fraction was washed in acetone to displace water and dried as a nominal quartz sample.

Clean 10 mm diameter stainless steel discs were prepared with one side sprayed with silicone grease as an adhesive layer, with sample material dispensed as a monolayer onto the central ~5 mm of the disc. For each sample, a pair of polymineral and a pair of quartz discs were dispensed.

2.2.2. Sample Measurement

Luminescence sensitivities (Photon Counts per Gy) and stored doses (Gy) were evaluated from paired aliquots of the polymineral and HF-etched quartz fractions, using Risø DA-15 automatic readers. The measurement cycles are summarised in Table 2.2.

For the quartz samples, measurements were conducted on an instrument equipped with a $^{90}Sr/^{90}Y$ β-source for irradiation, using blue LEDs emitting around 470 nm for optical stimulation, and a U340 detection filter pack to detect in the region 270-380 nm. Each measurement was preceded by a pre-heat at 200°C for 10s, with a 30s OSL measurement at 125°C. Measurements were conducted for the natural signal, and following nominal 5 Gy and 50 Gy irradiations, with all measurements accompanied by a nominal 1 Gy test dose.

For the polymineral samples, measurements were conducted on an instrument equipped with a $^{90}Sr/^{90}Y$ β-source for irradiation, infrared (laser) diodes emitting around 830 nm for optical stimulation, and a combination of Schott BG39 + Corning 7/59 + Schott GG400 filters. Each measurement was preceded by a pre-heat at 200°C for 10s, with a 30s IRSL measurement at 50°C and a TL measurement to 500°C. Measurements were conducted for the natural signal, and following nominal 5 Gy and 50 Gy irradiations. No test dose measurements were included.

Table 2.2: Summary of luminescence measurement procedure

Dose given	Quartz		Polymineral		
Natural	PH 200°C 10s	30s OSL at 125°C	PH 200°C 10s	30s IRSL at 50°C	TL to 500°C
TD1 (1 Gy)	PH 200°C 10s	30s OSL at 125°C	-	-	-
D1 (5 Gy)	PH 200°C 10s	30s OSL at 125°C	PH 200°C 10s	30s IRSL at 50°C	TL to 500°C
TD2 (1 Gy)	PH 200°C 10s	30s OSL at 125°C	-	-	-
D2 (50 Gy)	PH 200°C 10s	30s OSL at 125°C	PH 200°C 10s	30s IRSL at 50°C	TL to 500°C
TD3 (1 Gy)	PH 200°C 10s	30s OSL at 125°C	-	-	-
D3 (5 Gy)	PH 200°C 10s	30s OSL at 125°C	PH 200°C 10s	30s IRSL at 50°C	TL to 500°C
TD4 (1 Gy)	PH 200°C 10s	30s OSL at 125°C	-	-	-

For the OSL and IRSL signals, net counts were determined by summing the first 40 channels of stimulation, encompassing the majority of the peak, and subtracting the late light 40 channels of stimulation. For the TL signals, the counts between 300 and 500°C were integrated.

2.3. Dose Rate Determination

The three control samples contained sufficient material (>20 g) to allow dose rate determination using thick source beta counting (TSBC) and high resolution gamma spectrometry (HRGS).

Beta dose rates were measured directly using the SUERC TSBC system (Sanderson, 1988). Sample count rates were determined with six replicate 600 s counts for 20 g of each sample, bracketed by background measurements and sensitivity determinations using the Shap Granite secondary reference material. Infinite-matrix dose rates were calculated by scaling the net count rates of samples and reference material to the working beta dose rate of the Shap Granite (6.25 ± 0.03 mGy a^{-1}). The estimated errors combine counting statistics, observed variance and the uncertainty on the reference value.

Following TSBC, the 20 g samples were sealed using epoxy resin and left for three weeks to allow radon daughter equilibration. HRGS measurements were performed using a 50% relative efficiency "n" type hyper-pure Ge detector (EG&G Ortec Gamma-X) operated in a low background lead shield with a copper liner. Gamma ray spectra were recorded over the 30 keV to 3 MeV range from each sample, interleaved with background measurements and measurements from SUERC Shap Granite standard in the same geometries. Sample counts were made in duplicate over 80 ks. The spectra were analysed to determine count rates from the major line emissions from ^{40}K (1461 keV), and from selected nuclides in the U decay series (^{234}Th, ^{226}Ra + ^{235}U, ^{214}Pb, ^{214}Bi and ^{210}Pb) and the Th decay series (^{228}Ac, ^{212}Pb, ^{208}Tl) and their statistical counting uncertainties. Net rates and activity concentrations for each of these nuclides were determined relative to Shap Granite by weighted combination of the individual lines for each nuclide. The internal consistency of nuclide specific estimates for U and Th decay series nuclides was assessed relative to measurement precision, and weighted combinations used to estimate mean activity concentrations (Bq kg^{-1}) and elemental concentrations (% K and ppm U, Th) for the parent activity. These data were used to determine infinite matrix dose rates for alpha, beta and gamma radiation.

The dose rate measurements were used, in combination with the grain size and assumed burial water contents, to determine the overall effective dose rates for age estimation. Cosmic dose rates were modelled by combining latitude and altitude specific dose rates for the site with corrections for estimated depth of overburden using the method of Prescott and Hutton (1994).

2.4. Quartz SAR luminescence measurements

For the three profile samples corresponding to the control samples (SUTL2969/1, SUTL2969/9 and SUTL2969/17) further minerals were extracted and quartz grains purified for dose determination using a single aliquot regenerative (SAR) procedure.

2.4.1. Sample Preparation

Approximately 5 g of material was removed for each sample and processed to obtain sand-sized quartz grains for luminescence measurements. Each sample was wet sieved to obtain the 90-150 and 150-250 μm fractions. The 150-250 μm fractions were treated with 1 M hydrochloric acid (HCl) for 10 minutes, 15% hydrofluoric acid (HF) for 15 minutes, and 1 M HCl for a further 10 minutes. The HF-etched sub-samples were then centrifuged in sodium polytungstate solutions of ~2.64, and 2.74 g cm^{-3}, to obtain concentrates of feldspars (<2.64 g cm^{-3}), and quartz plus plagioclase (2.64-2.74 g cm^{-3}). The selected quartz fraction was then subjected to further HF and HCl washes (40% HF for 40 mins, followed by 1M HCl for 10 mins).

All materials were dried at 50°C and transferred to Eppendorf tubes. The 40% HF-etched, 2.64-2.74 g cm^{-3} 'quartz' 150-250 μm fractions were dispensed to 10 mm stainless steel discs for measurement. 16 aliquots were dispensed for each sample. The purity of which was checked using a Hitachi S-3400N scanning electron microscope (SEM), coupled with an Oxfords Instruments INCA EDX system, to determine approximate elemental concentrations for each sample.

2.4.2. SAR measurements

All measurements were conducted using a Risø DA-15 automatic reader equipped with a $^{90}Sr/^{90}Y$ β-source for irradiation, blue LEDs emitting around 470 nm and infrared (laser) diodes emitting around 830 nm for optical stimulation, and a U340 detection filter pack to detect in the region 270-380 nm, while cutting out stimulating light (Bøtter-Jensen et al., 2000).

Equivalent dose determinations were made on sets of 16 aliquots per sample, using a single aliquot regeneration (SAR) sequence (cf Murray and Wintle, 2000). Using this procedure, the OSL signal levels from each individual disc were calibrated to provide an absorbed dose estimate (the equivalent dose) using an interpolated dose-response curve, constructed by regenerating OSL signals by beta irradiation in the laboratory. Sensitivity changes which may occur as a result of readout, irradiation and preheating (to remove unstable radiation-induced signals) were monitored using small test doses after each regenerative dose. Each measurement was standardised to the test dose response determined immediately after its readout, to compensate for changes in

sensitivity during the laboratory measurement sequence. The regenerative doses were chosen to encompass the likely value of the equivalent (natural) dose. A repeat dose point was included to check the ability of the SAR procedure to correct for laboratory-induced sensitivity changes (the 'recycling test'), a zero dose point is included late in the sequence to check for thermally induced charge transfer during the irradiation and preheating cycle (the 'zero cycle'), and an IR response check included to assess the magnitude of non-quartz signals. Regenerative dose response curves were constructed using nominal doses of 1.0, 5.0, 10, 20 and 30 Gy, with test doses of 1.0 Gy. A dose recovery test is included that uses the first test dose, normalised by the following 1 Gy regenerative dose, as the "natural" signal. The 16 aliquot sets were sub-divided into four subsets of four aliquots, such that four preheating regimes were explored (220°C, 240°C, 260°C and 280°C).

3. Results

3.1. Portable OSL Measurements

The portable instrument measurements are shown in Figure 3.1, and tabulated in the appendix. These show a general increase in net counts for both the blue and IR stimulated signals, which does not reproduce the inversion observed from the Thailand samples (Figure 1.1). The IRSL counts are 2-3 orders of magnitude smaller than OSL counts. OSL depletion ratios are significantly larger than would normally be expected, with the lower four samples having ratios of ~4 compared to ~3.5 for the rest of the profile, which may be indicative of a different source of quartz for these lower samples. The bright OSL signals and very high depletion ratios are similar to other samples from Thailand and Cambodia (Sanderson et.al. 2003, 2007), and suggest that these samples contain significant proportions of bright quartz that was well zeroed at time of deposition. IRSL depletion ratios are generally in the range of 1.4-1.9. The IRSL:OSL ratio increases down the core, whereas it would normally be expected to decrease as the contribution from more easily weathered feldspars in older sediments decreases.

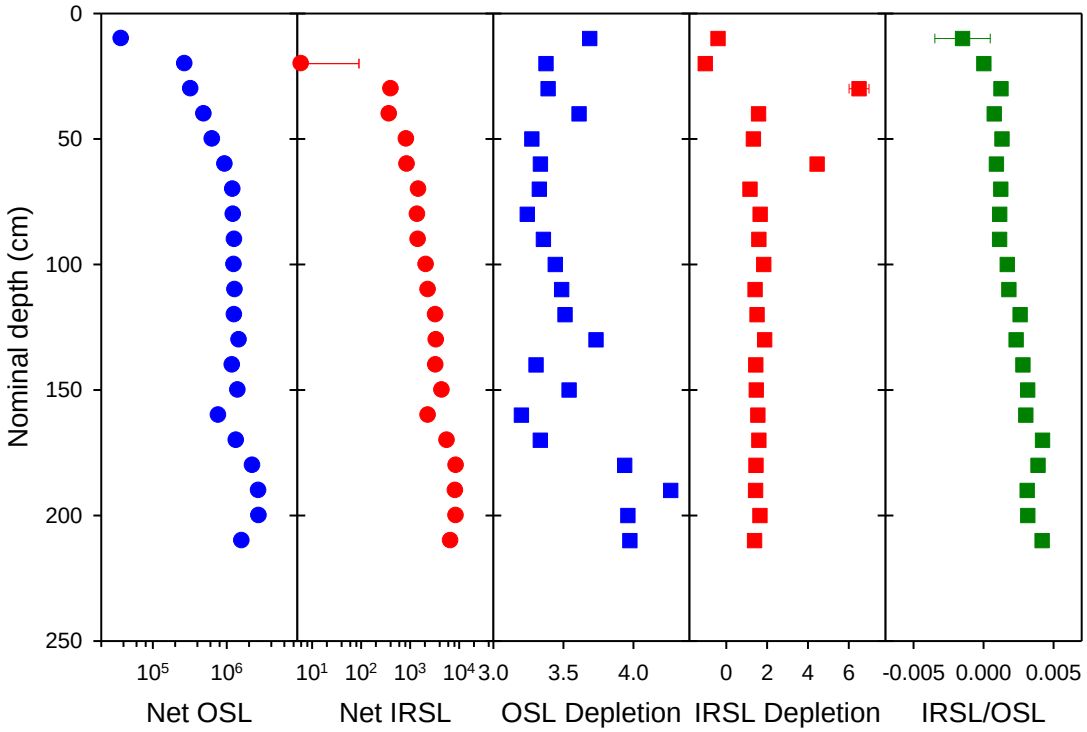

Figure 3.1: Portable instrument measurements showing net counts and depletion ratios for OSL and IRSL, and the IRSL to OSL ratio.

3.2. Laboratory Profiling Measurements

The results of the laboratory profiling measurements for the 21 samples of SUTL2969 are plotted in Figure 3.2, with the values tabulated in Appendix A.

The stored dose estimates by all three methods follow a similar trend, increasing with depth, which reflects the portable net count measurements (Figure 3.1). The sensitivities show no significant trend with depth, with the OSL measurements of quartz 2-3 orders of magnitude more sensitive than the IRSL measurements of polymineral grains, similar to the difference between OSL and IRSL net counts for the portable measurements.

The OSL stored dose estimates show what appear to be three subtly different zones. The top 6-7 samples show a steady increase in stored dose for approximately 0 Gy to approximately 12 Gy. Below which is a zone of 7-8 samples with approximately constant stored doses of 12-15 Gy. Then there is a discontinuity with the lower 7 samples with doses of approximately 25 Gy. The IRSL and TL (300-500°C) dose estimates are smaller than the OSL values, by a factor of approximately 2-3. For the IRSL the top samples, corresponding to the top zone of increasing dose in the OSL data, has low doses that increase slowly, thereafter the dose estimates increase steadily with depth. For the TL data, there is a steady increase in dose estimate with depth, with the bottom 7-8 samples below the discontinuity noticed in the OSL data increasing in dose more slowly.

The absence of large geological doses in the TL signal indicates that these sediments were very well bleached prior to deposition, given that TL signals are expected to be far harder to remove than OSL or IRSL.

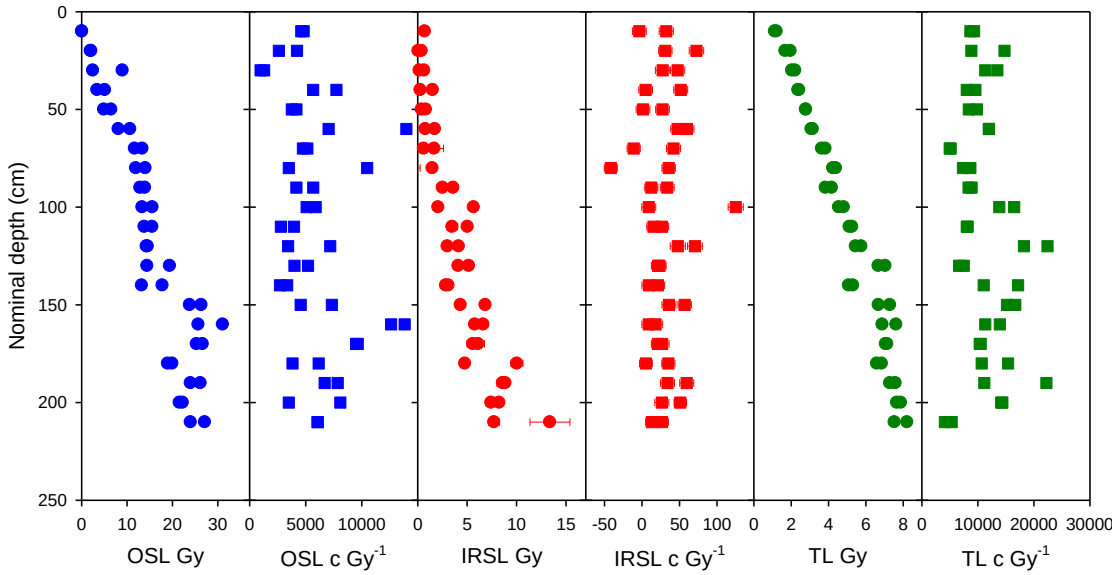

Figure 3.2: Laboratory luminescence profile measurement results showing estimated stored dose (Gy) and measured sensitivity (c Gy^{-1}) for OSL measurements on quartz grains and IRSL and TL measurements on polymineral grains.

Comparisons between the estimated stored doses for the control samples (SUTL2970) compared to the corresponding profile sample (SUTL2969) are given in Table 3.1. It can be seen that the 2h exposure to strong daylight removed >80% of the OSL and IRSL signals, without significantly bleaching the TL (300-500°C) signals. The dose estimates for the OSL and IRSL measurements of 0.7-2.6 Gy (OSL) and 0-0.5 Gy (IRSL) are significantly larger than would be expected from transit doses and suggest that the 2h of daylight exposure is insufficient to fully bleach these signals.

Table 3.1: Percentage of signal remaining in control samples following 2h exposure to strong daylight.

Control Sample	Profile Sample	% OSL remaining	% IRSL remaining	% TL remaining
SUTL2970A	SUTL2969/1	3.0 ± 0.2	5.2 ± 1.5	95.7 ± 0.3
SUTL2970B	SUTL2969/9	15.5 ± 0.5	8.9 ± 5.3	100.9 ± 0.3
SUTL2970C	SUTL2969/17	20.5 ± 0.8	-3.9 ± 5.0	91.1 ± 0.3

3.3. Dose Rate Measurements

HRGS results are shown in Table 3.2, both as activity concentrations (i.e. disintegrations per second per kilogram) and as equivalent parent element concentrations (in % and ppm), based in the case of U and Th on combining nuclide specific data assuming decay series equilibrium.

Table 3.2: Activity and equivalent concentrations of K, U and Th determined by HRGS

SUTL no.	Activity Concentration[a] / Bq kg^{-1}			Equivalent Concentration[b]		
	K	U	Th	K / %	U / ppm	Th / ppm
2970A	160 ± 33	41.9 ± 2.7	41.0 ± 2.0	0.52 ± 0.11	3.39 ± 0.22	10.10 ± 0.50
2970B	126 ± 32	28.4 ± 2.6	34.0 ± 1.9	0.41 ± 0.10	2.30 ± 0.21	8.39 ± 0.47
2970C	66 ± 35	26.3 ± 2.5	23.4 ± 1.9	0.21 ± 0.11	2.13 ± 0.21	5.77 ± 0.48

[a]Shap granite reference, working values determined by David Sanderson in 1986, based on HRGS relative to CANMET and NBL standards.

[b]Activity and equivalent concentrations for U, Th and K determined by HRGS (Conversion factors based on NEA (2000) decay constants): 40K: 309.3 Bq kg^{-1} %K^{-1}, 238U: 12.35 Bq kg^{-1} ppmU^{-1}, 232Th: 4.057 Bq kg^{-1} ppm Th^{-1}

Infinite matrix alpha, beta and gamma dose rates from HRGS are listed for all samples in Table 3.3, together with infinite matrix beta dose rates from TSBC. The gamma spectrometry shows no evidence of disequilibrium in the samples, nor anomalous U:Th ratios, which is supported by the TSBC giving data consistent with the values calculated from the HRGS data. The dry beta dose rates carried forward to calculate effective dose rates are the mean of the HRGS and TSBC values.

Table 3.3: Infinite matrix dose rates determined by HRGS and TSBC

SUTL no.	HRGS, dry[a] / mGy a^{-1}			TSBC, dry / mGy a^{-1}
	Alpha	Beta	Gamma	
2970A	16.89 ± 0.71	1.21 ± 0.10	1.03 ± 0.04	1.05 ± 0.05
2970B	12.59 ± 0.68	0.91 ± 0.09	0.79 ± 0.04	0.92 ± 0.05
2970C	10.19 ± 0.67	0.65 ± 0.10	0.59 ± 0.04	0.55 ± 0.04

[a]based on dose rate conversion factors in Aikten (1983) and Sanderson (1987)

Effective dose rates to the HF-etched 150-250 μm quartz grains are given in Table 3.4 (the mean of the TSBC and HRGS data, accounting for water content and grain size), together with the estimate of the gamma dose rate (HRGS data, accounting for water content), and the total dose rate (the sum of effective beta and gamma dose rates, and the cosmic dose rate). Water content had not been measured for these samples, and an assumed 15 ± 10% has been applied. A cosmic dose rate of 0.185 mGy a^{-1} has been used.

Table 3.4: Effective beta and gamma dose rates following water correction.

SUTL no.	Effective Dose Rate / mGy a^{-1}		
	Beta[a]	Gamma	Total[b]
2970A	0.89 ± 0.12	0.89 ± 0.09	1.96 ± 0.15
2970B	0.67 ± 0.10	0.68 ± 0.07	1.53 ± 0.12
2970C	0.47 ± 0.09	0.51 ± 0.06	1.17 ± 0.11

[a] Effective beta dose rate combining water content corrections with inverse grain size attenuation factors obtained by weighting the 150-250 μm attenuation factors of Mejdahl (1979) for K, U, and Th by the relative beta dose contributions for each source determined by Gamma Spectrometry;
[b] includes a cosmic dose contribution

3.4. Quartz single aliquot equivalent dose determinations

For equivalent dose determination, data from single aliquot regenerative dose measurements were analysed using the Risø TL/OSL Viewer programme to export integrated summary files that were analysed in MS Excel and SigmaPlot. Composite dose response curves were constructed from selected discs and when possible, for each of the preheating groups from each sample, and used to estimate equivalent dose values for each individual disc and their combined sets. Dose response curves (shown in Appendix B) for each of the preheating temperature groups and the combined data were determined using a fit to a saturating exponential function. Probability density functions (PDFs), Kernel Density Estimate (KDE) and abanico plots were generated to describe the dose distributions, and are also shown in Appendix B.

SAR quality parameters are given in Table 3.5. For the upper two samples (SUTL2969/9 and 2969/17) the sensitivity is ~3000 c Gy^{-1}, the lower sample (SUTL2969/1) has significantly lower sensitivity. All samples show a small increase in sensitivity of 2-6% per cycle, negligible IRSL signals and no signal for the zero cycle. Recycling ratios and dose recovery tests produce values that are unity within uncertainties (except for the SUTL2969/17 dose recovery test which is unity within 3σ).

Table 3.5: SAR quality parameters

SUTL no.	Mean sensitivity c Gy^{-1}	Sensitivity change / cycle (%)	Recycling ratio	Zero cycle	Dose recovery	IRSL (%)
2969/1	810 ± 90	2.2 ± 3.4	0.96 ± 0.04	-0.12 ± 0.04	1.03 ± 0.06	-1.5 ± 1.6
2969/9	3229 ± 289	5.8 ± 3.2	0.98 ± 0.04	0.01 ± 0.01	1.02 ± 0.02	0.1 ± 0.3
2969/17	2694 ± 189	4.1 ± 2.3	1.03 ± 0.02	-0.01 ± 0.01	1.06 ± 0.02	-0.2 ± 0.3

For each sample, the mean, weighted mean and a robust mean were calculated, as given in Table 3.6, with the equivalent dose estimated from the profile measurements (Table A.2) for comparison. The SAR procedure used was conducted with regenerative doses up to a nominal 30 Gy. The measurements for SUTL2969/1 showed a significant number of aliquots with normalised natural counts in excess of the normalised counts for 30 Gy and the saturation value from an exponential rise through the data points. For this sample, additional regenerative dose points were added at nominal doses of 50, 75, 100 and 200 Gy. This improves the constraint on the saturation counts for the rising exponential fit, with the curve (Fig. B.1) saturating above 100 Gy. Some aliquots still exceed this saturation value, and there is a hint in the data of a continuing slow growth in signal beyond 100 Gy. These would correspond to aliquots with an equivalent dose significantly in excess of 100 Gy, but the precision of any value determined would be very poor. For SUTL2969/1 and 2969/9 the equivalent dose distributions show a dominant peak, with a tail to higher doses, and for 2969/17 a single very broad peak. In all cases the weighted mean approximates to the dominant peak, favouring the higher precision lower dose data, with the mean and robust mean giving higher values. The weighted mean is thus taken as being the best value for the equivalent dose for each sample. The extension on the regenerative dose range for SUTL2969/1 has resulted in a small change in the equivalent dose estimate, but with more data contributing this is now higher precision. The SAR equivalent doses for SUTL2969/9 and 2969/17 show an inversion, with the upper sample carrying a significantly larger dose, which is not evident in the profiling measurements.

Table 3.6: Comments on equivalent dose distributions; mean values with preferred estimates in bold, and the corresponding estimates from profile measurements.

SUTL no.	Comments on stored dose distribution / individual samples	Mean	Weighted Mean	Robust Mean	Profile
2969/1	9 saturated aliquots. 3 aliquots fail SAR quality checks. 4 aliquots form single peak at ~30 Gy	35.8 ± 2.3	29.0 ± 4.1	35.8 ± 0.6	25.6 ± 0.5
	Eight aliquots forming a broad peak 10-40 Gy, remaining aliquots >100 Gy with very poor precision	56.9 ± 8.8	**28.2 ± 2.0**	51.0 ± 2.5	
2969/9	A dominant peak at ~10 Gy, with tail to ~40 Gy	13.0 ± 1.8	**8.2 ± 0.2**	11.7 ± 0.3	16.9 ± 0.4
2969/17	Broad distribution of peaks from 5-50 Gy, with four aliquots saturated (>100 Gy)	27.6 ± 2.4	**18.8 ± 0.7**	27.6 ± 0.2	5.71 ± 0.12

errors stated: ± weighted standard deviation (weighted error)
SUTL2969/1: top line is for the initial SAR measurements; bottom line for the extended dose range.

The calculated ages for these samples are given in Table 3.7, combining the preferred stored dose estimate (Table 3.6) with the total dose rate from the corresponding control sample (Table 3.4).

Table 3.7: Quartz OSL ages

SUTL no.	Dose (Gy)	Dose Rate (mGy a^{-1})	Years / ka
2969/1	28.2 ± 2.0	1.96 ± 0.15	14.4 ± 2.1
2969/9	8.2 ± 0.2	1.53 ± 0.12	5.4 ± 0.7
2969/17	18.8 ± 0.7	1.17 ± 0.11	16.0 ± 2.3

By assuming the dose rates measured for each of the three samples is representative of the dose rate for sampling locations within ~50 cm of them, the dose estimates from the profile samples (Table A.2, Fig. 3.2) can be used to determine apparent ages for the profile samples. These are plotted in Fig. 3.3 with the quartz OSL ages (Table 3.7).

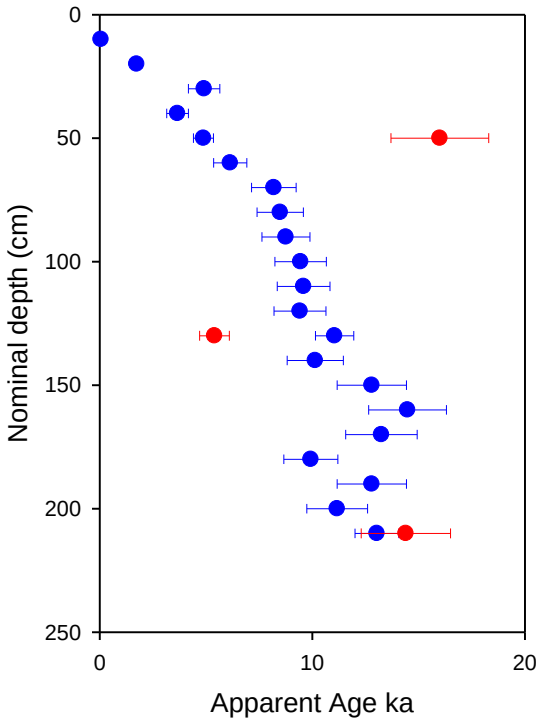

Figure 3.3: Apparent ages from profile measurements (blue) with OSL SAR ages (red)

4. Discussion and conclusions

To further investigate an inversion in luminescence counts observed from a profile collected in Thailand a further profile from the same stratigraphic horizon has been collected from Vietnam. Luminescence measurements using both a portable instrument measuring bulk samples and laboratory instruments on separated 90-250 µm polymineral and acid etched quartz grains show bright OSL signals which do not reproduce the inversion previously observed.

The luminescence measurements show that these materials had been very well bleached prior to deposition, removing signals associated with the hard to bleach TL (300-500°C) traps as well as the more readily bleached optical traps. The control samples, which had been exposed to strong daylight for 2h, showed significant but incomplete bleaching of optical signals with no significant reduction in TL signals.

The luminescence profiles suggest that there are three distinct zones within the sedimentary sequence. At the top, the youngest 6-7 samples show a steady increase in stored dose estimates from OSL measurements on quartz (from 0 to ~12 Gy), with a slow increase from polymineral IRSL. The middle 7-8 samples show approximately constant quartz OSL dose estimates (12-15 Gy) with a more rapid increase in polymineral IRSL estimates. There is a discontinuity in quartz OSL dose between the middle zone and the lower, oldest 7-8 samples. These show a higher quartz OSL dose of ~25 Gy, with a reduced rate of increase in polymineral TL stored dose and also a higher OSL depletion rate and IRSL:OSL ratio measured with the portable instrument.

The data suggest a history with a period of rapid sedimentation depositing the lower zone, followed by an erosional event that removed the upper part of this sequence. A second period of rapid sedimentation with material which has a lower OSL depletion rate and IRSL:OSL ratio then produced the middle zone. Finally a more recent period of slower sedimentation produced the upper zone with steadily increasing stored dose.

Dose rates of ~0.9-1.0 mGy a^{-1} have been estimated for quartz rich sediments in Thailand (Sanderson et.al. 2001). The three control samples supplied contained sufficient material for dose rate estimation. These give dose rates of 1.2-2.0 mGy a^{-1}, with higher dose rates for the sample at the bottom of the sequence, and lowest dose rate at the top. These variations in dose rate will reflect the mineralogy of the sediments, indicating that the source materials for the three zones are possibly different.

The three samples corresponding to the three control samples were processed for quantitative SAR OSL dating, with etched 150-250 µm quartz grains extracted. The upper two samples show a greater sensitivity from the lower sample, by a factor of 3-4. This difference in sensitivity is not evident in the profiling measurements. Again this suggests a different provenance for the quartz in the lower zone of the sedimentary sequence.

The upper two samples show an age inversion that was not suggested by the profile measurements. For the lower sample this produces an age of 14 ± 2 ka, within the range of values for the OSL dates of two samples for the corresponding layer in

Thailand (8 and 19 ka). However, it is noted that this sample also contains material with a very much older age (significantly in excess of 50 ka), which cannot be reliably dated using the SAR approach adopted here. Alternative approaches to luminescence analysis of quartz (eg: TT-OSL) could be used on material from this sample, or samples collected in the future, to provide ages for these older components, which could help address the question of whether the 8-19 ka ages obtained reflect the depositional date for these sediments or subsequent disturbance introducing younger material.

References

Aitken, M.J., 1983, Dose rate data in SI units: PACT, v. 9, p. 69–76.

Burbidge, C.I., Sanderson, D.C.W., Housley, R.A. and Allsworth Jones, P. 2007. Survey of Palaeolithic sites by luminescence profiling, a case study from Eastern Europe. *Quaternary Geochronology*, **2**, p. 296-302.

Mejdahl, V., 1979, Thermoluminescence daing: Beta-dose attenuation in quartz grains Archaeometry, v. 21, p. 61-72.

Mejdahl, V., 1983, Feldspar inclusion dating of ceramics and burnt stones, PACT, v. 9, p. 351-364.

NEA, 2000, The JEF-2.2 Nuclear Data Library: Nuclear Energy Agency, Organisation for economic Co-operation and Development. JEFF Report, v. 17.

Prescott, J.R., and Hutton, J.T., 1994, Cosmic ray contributions to dose rates for luminescence and ESR dating: Large depths and long-term time variations: Radiation Measurements, v. 23, p. 497-500.

Sanderson, D.C.W., 1987, Thermoluminescence dating of vitrified Scottish Forts: Paisley, Paisley college.

—, 1988, Thick source beta counting (TSBC): A rapid method for measuring beta dose-rates: International Journal of Radiation Applications and Instrumentation. Part D. Nuclear Tracks and Radiation Measurements, v. 14, p. 203-207.

Sanderson, D.C.W., Bishop, P., Houston, I. and Boonsener, M. 2001. Luminescence characterisation of quartz-rich cover sands from NE Thailand. *Quaternary Science Reviews*, **20**, p. 893-900.

Sanderson, D.C.W., Bishop, P., Stark, M.T., Spencer, J.Q., 2003, Luminescence dating of anthropogenically reset canal sediments from Angkor Borei, Mekong Delta, Cambodia. Quaternary Science Reviews 22, 1111–1121.

Sanderson, D.C.W., Bishop, P., Stark, M., Alexander, S. and Penny, D. 2007. Luminescence dating of canal sediments from Angkor Borei, Mekong Delta, Southern Cambodia. *Quaternary Geochronology*, **2**, p. 322-329.

Sanderson, D.C.W., and Murphy, S., 2010, Using simple portable OSL measurements and laboratory characterisation to help understand complex and heterogeneous sediment sequences for luminescence dating: Quaternary Geochronology, v. 5, p. 299-305.

Appendix A: Luminescence Profiling Results

Table A.1: Portable instrument measurements

	IRSL		OSL		
Sample	Net counts	Depletion ratio	Net counts	Depletion ratio	IRSL:OSL
SUTL2969/1	6672 ± 103	1.38 ± 0.04	1594680 ± 1266	3.975 ± 0.008	0.0042 ± 0.0001
SUTL2969/2	8575 ± 121	1.65 ± 0.04	2716806 ± 1652	3.960 ± 0.006	0.0032 ± 0.0001
SUTL2969/3	8373 ± 114	1.43 ± 0.03	2686441 ± 1642	4.266 ± 0.007	0.0031 ± 0.0001
SUTL2969/4	8652 ± 116	1.46 ± 0.03	2225879 ± 1495	3.937 ± 0.007	0.0039 ± 0.0001
SUTL2969/5	5648 ± 104	1.60 ± 0.05	1342570 ± 1162	3.335 ± 0.007	0.0042 ± 0.0001
SUTL2969/6	2321 ± 74	1.54 ± 0.08	769692 ± 881	3.200 ± 0.009	0.0030 ± 0.0001
SUTL2969/7	4438 ± 89	1.47 ± 0.05	1408232 ± 1190	3.541 ± 0.007	0.0032 ± 0.0001
SUTL2969/8	3332 ± 84	1.44 ± 0.06	1185671 ± 1093	3.305 ± 0.007	0.0028 ± 0.0001
SUTL2969/9	3408 ± 102	1.88 ± 0.07	1464629 ± 1214	3.733 ± 0.008	0.0023 ± 0.0001
SUTL2969/10	3299 ± 85	1.51 ± 0.06	1265141 ± 1128	3.512 ± 0.008	0.0026 ± 0.0001
SUTL2969/11	2323 ± 83	1.41 ± 0.06	1288614 ± 1139	3.487 ± 0.007	0.0018 ± 0.0001
SUTL2969/12	2110 ± 84	1.84 ± 0.09	1248451 ± 1121	3.442 ± 0.007	0.0017 ± 0.0001
SUTL2969/13	1456 ± 91	1.60 ± 0.07	1270442 ± 1132	3.357 ± 0.007	0.0011 ± 0.0001
SUTL2969/14	1406 ± 78	1.66 ± 0.09	1222787 ± 1110	3.242 ± 0.007	0.0011 ± 0.0001
SUTL2969/15	1480 ± 72	1.16 ± 0.07	1202699 ± 1101	3.328 ± 0.007	0.0012 ± 0.0001
SUTL2969/16	861 ± 90	4.45 ± 0.23	941457 ± 975	3.336 ± 0.008	0.0009 ± 0.0001
SUTL2969/17	835 ± 68	1.33 ± 0.10	634589 ± 800	3.275 ± 0.010	0.0013 ± 0.0001
SUTL2969/18	374 ± 83	1.58 ± 0.10	489312 ± 704	3.612 ± 0.013	0.0008 ± 0.0002
SUTL2969/19	405 ± 75	6.50 ± 0.49	324669 ± 574	3.391 ± 0.014	0.0012 ± 0.0002
SUTL2969/20	6 ± 84	-1.03 ± 0.07	269728 ± 525	3.376 ± 0.016	0.0000 ± 0.0003
SUTL2969/21	-56 ± 74	-0.40 ± 0.03	37305 ± 206	3.688 ± 0.049	-0.0015 ± 0.0020
SUTL2970A	-451 ± 103	-1.49 ± 0.11	27930 ± 199	2.130 ± 0.028	-0.0161 ± 0.0037
SUTL2970B	342 ± 84	-29.5 ± 1.82	53596 ± 244	2.959 ± 0.030	0.0064 ± 0.0016
SUTL2970C	206 ± 67	0.16 ± 0.02	39552 ± 210	3.012 ± 0.036	0.0052 ± 0.0017

Table A.2: Results of OSL profiling of quartz fractions, for each aliquot and the mean values. Showing sensitivity (from TD1 response), sensitivity change (ratio of TD4 to TD1) and dose estimates (from natural and D1 normalised responses).

Sample	Sensitivity c Gy^{-1}			Sensitivity change			Dose estimate Gy		
	Al 1	Al 2	Mean	Al 1	Al 2	Mean	Al 1	Al 2	Mean
SUTL2969/1	6060 ± 109	6069 ± 99	6065 ± 74	0.637 ± 0.020	0.539 ± 0.017	0.588 ± 0.013	24.00 ± 0.70	27.13 ± 0.74	25.57 ± 0.51
SUTL2969/2	3493 ± 86	8091 ± 114	5792 ± 72	0.610 ± 0.030	0.602 ± 0.015	0.606 ± 0.017	21.56 ± 0.90	22.24 ± 0.52	21.90 ± 0.52
SUTL2969/3	6690 ± 99	7853 ± 105	7272 ± 72	0.628 ± 0.016	0.675 ± 0.015	0.652 ± 0.011	26.18 ± 0.62	24.01 ± 0.52	25.09 ± 0.40
SUTL2969/4	6160 ± 104	3824 ± 83	4992 ± 67	0.640 ± 0.019	0.573 ± 0.025	0.606 ± 0.016	18.98 ± 0.54	19.96 ± 0.73	19.47 ± 0.45
SUTL2969/5	9498 ± 112	9644 ± 115	9571 ± 80	0.673 ± 0.013	0.624 ± 0.013	0.648 ± 0.009	25.32 ± 0.48	26.64 ± 0.51	25.98 ± 0.35
SUTL2969/6	12616 ± 134	13830 ± 138	13223 ± 96	0.624 ± 0.012	0.579 ± 0.010	0.602 ± 0.008	31.07 ± 0.52	25.69 ± 0.41	28.38 ± 0.33
SUTL2969/7	7338 ± 101	4549 ± 88	5943 ± 67	0.612 ± 0.015	0.653 ± 0.023	0.632 ± 0.014	23.81 ± 0.53	26.36 ± 0.80	25.09 ± 0.48
SUTL2969/8	3346 ± 78	2713 ± 78	3029 ± 55	0.963 ± 0.035	0.707 ± 0.037	0.835 ± 0.025	13.24 ± 0.48	17.78 ± 0.81	15.51 ± 0.47
SUTL2969/9	5213 ± 89	3999 ± 81	4606 ± 60	0.651 ± 0.020	0.675 ± 0.024	0.663 ± 0.016	19.40 ± 0.52	14.43 ± 0.49	16.91 ± 0.36
SUTL2969/10	7189 ± 100	3430 ± 81	5309 ± 64	0.658 ± 0.016	0.688 ± 0.028	0.673 ± 0.016	14.30 ± 0.32	14.54 ± 0.59	14.42 ± 0.33
SUTL2969/11	3955 ± 78	2786 ± 71	3371 ± 53	0.769 ± 0.026	0.810 ± 0.035	0.790 ± 0.022	15.55 ± 0.52	13.81 ± 0.56	14.68 ± 0.38
SUTL2969/12	5087 ± 84	5888 ± 94	5488 ± 63	0.709 ± 0.020	0.736 ± 0.019	0.723 ± 0.014	13.35 ± 0.36	15.57 ± 0.39	14.46 ± 0.27
SUTL2969/13	5671 ± 84	4172 ± 75	4922 ± 57	0.643 ± 0.017	0.761 ± 0.023	0.702 ± 0.014	13.93 ± 0.34	12.89 ± 0.38	13.41 ± 0.25
SUTL2969/14	3495 ± 76	10487 ± 112	6991 ± 68	0.773 ± 0.029	0.628 ± 0.012	0.701 ± 0.016	11.95 ± 0.42	14.04 ± 0.24	12.99 ± 0.24
SUTL2969/15	5151 ± 84	4753 ± 82	4952 ± 59	0.702 ± 0.020	0.834 ± 0.024	0.768 ± 0.015	13.37 ± 0.36	11.70 ± 0.32	12.53 ± 0.24
SUTL2969/16	7048 ± 95	13980 ± 126	10514 ± 79	0.736 ± 0.017	0.707 ± 0.011	0.721 ± 0.010	8.11 ± 0.18	10.68 ± 0.16	9.40 ± 0.12
SUTL2969/17	3760 ± 71	4171 ± 74	3966 ± 51	0.756 ± 0.024	0.883 ± 0.025	0.820 ± 0.017	4.92 ± 0.15	6.50 ± 0.19	5.71 ± 0.12
SUTL2969/18	5669 ± 84	7746 ± 96	6708 ± 64	0.955 ± 0.022	0.799 ± 0.016	0.877 ± 0.014	3.43 ± 0.08	5.12 ± 0.10	4.28 ± 0.07
SUTL2969/19	977 ± 51	1290 ± 53	1134 ± 37	1.154 ± 0.087	1.052 ± 0.065	1.103 ± 0.054	8.99 ± 0.72	2.49 ± 0.16	5.74 ± 0.37
SUTL2969/20	4228 ± 75	2610 ± 65	3419 ± 50	0.825 ± 0.024	0.932 ± 0.038	0.878 ± 0.022	2.10 ± 0.06	1.98 ± 0.08	2.04 ± 0.05
SUTL2969/21	4610 ± 77	4813 ± 78	4712 ± 55	0.997 ± 0.026	1.309 ± 0.030	1.153 ± 0.020	0.07 ± 0.01	0.06 ± 0.01	0.07 ± 0.01
SUTL2970A	3324 ± 72	6771 ± 98	5047 ± 61	0.682 ± 0.026	0.700 ± 0.018	0.691 ± 0.016	0.24 ± 0.02	1.27 ± 0.03	0.76 ± 0.02
SUTL2970B	14335 ± 133	11627 ± 119	12981 ± 89	0.731 ± 0.011	0.707 ± 0.012	0.719 ± 0.008	2.37 ± 0.04	2.86 ± 0.05	2.61 ± 0.03
SUTL2970C	6297 ± 86	3634 ± 73	4965 ± 57	0.752 ± 0.018	0.874 ± 0.029	0.813 ± 0.017	2.11 ± 0.05	0.23 ± 0.02	1.17 ± 0.03

Table A.3: Results of IRSL profiling of polymineral fractions, for each aliquot and the mean values. Showing sensitivity (from D1 response), sensitivity change (ratio of D3 to D1) and dose estimates (from natural and D2 responses).

Sample	Sensitivity c Gy^{-1}			Sensitivity change			Dose estimate Gy		
	Al 1	Al 2	Mean	Al 1	Al 2	Mean	Al 1	Al 2	Mean
SUTL2969/1	13.0 ± 8.3	26.4 ± 8.7	19.7 ± 6.0	-0.242 ± 0.710	0.508 ± 0.377	0.133 ± 0.402	13.38 ± 2.02	7.72 ± 0.56	10.55 ± 1.05
SUTL2969/2	26.4 ± 9.4	51.0 ± 8.3	38.7 ± 6.2	2.310 ± 0.896	0.494 ± 0.198	1.402 ± 0.459	8.25 ± 0.40	7.43 ± 0.55	7.84 ± 0.34
SUTL2969/3	34.0 ± 9.3	59.6 ± 9.4	46.8 ± 6.6	1.370 ± 0.459	0.363 ± 0.172	0.867 ± 0.245	8.60 ± 0.58	8.86 ± 0.35	8.73 ± 0.34
SUTL2969/4	35.1 ± 8.8	5.2 ± 8.5	20.2 ± 6.1	1.174 ± 0.392	3.720 ± 6.308	2.447 ± 3.160	10.04 ± 0.6	4.78 ± 0.33	7.41 ± 0.34
SUTL2969/5	21.2 ± 8.7	26.9 ± 9.2	24.0 ± 6.4	0.792 ± 0.541	0.156 ± 0.335	0.474 ± 0.318	6.12 ± 0.64	5.58 ± 0.59	5.85 ± 0.44
SUTL2969/6	9.0 ± 9.1	18.1 ± 9.5	13.5 ± 6.6	5.767 ± 5.891	0.593 ± 0.598	3.180 ± 2.960	5.78 ± 0.34	6.62 ± 0.47	6.20 ± 0.29
SUTL2969/7	35.9 ± 9.3	56.9 ± 8.9	46.4 ± 6.5	1.906 ± 0.559	0.745 ± 0.202	1.326 ± 0.297	6.84 ± 0.28	4.33 ± 0.23	5.59 ± 0.18
SUTL2969/8	21.2 ± 9.0	9.2 ± 9.3	15.2 ± 6.5	1.079 ± 0.642	4.682 ± 4.805	2.881 ± 2.424	2.85 ± 0.22	3.10 ± 0.16	2.97 ± 0.14
SUTL2969/9	23.3 ± 8.8	21.4 ± 8.9	22.4 ± 6.3	0.541 ± 0.435	1.882 ± 0.892	1.211 ± 0.496	5.17 ± 0.44	4.10 ± 0.31	4.63 ± 0.27
SUTL2969/10	47.7 ± 10.1	70.5 ± 9.8	59.1 ± 7.1	1.537 ± 0.385	1.188 ± 0.217	1.362 ± 0.221	4.14 ± 0.17	3.00 ± 0.12	3.57 ± 0.10
SUTL2969/11	15.3 ± 8.9	26.7 ± 8.8	21.0 ± 6.2	1.041 ± 0.835	0.189 ± 0.334	0.615 ± 0.450	5.04 ± 0.37	3.49 ± 0.54	4.27 ± 0.33
SUTL2969/12	9.0 ± 9.3	124.9 ± 10.1	67.0 ± 6.9	4.581 ± 4.838	0.713 ± 0.101	2.647 ± 2.419	2.07 ± 0.14	5.66 ± 0.16	3.87 ± 0.11
SUTL2969/13	33.6 ± 9.2	12.4 ± 8.7	23.0 ± 6.3	0.806 ± 0.354	1.729 ± 1.406	1.268 ± 0.725	2.52 ± 0.19	3.59 ± 0.33	3.05 ± 0.19
SUTL2969/14	-41.6 ± 8.7	35.5 ± 8.9	-3.0 ± 6.2	-0.667 ± 0.250	0.769 ± 0.318	0.051 ± 0.202	-0.08 ± 0.32	1.48 ± 0.30	0.70 ± 0.22
SUTL2969/15	-11.1 ± 8.8	42.0 ± 9.4	15.4 ± 6.4	-0.604 ± 0.925	0.095 ± 0.214	-0.254 ± 0.475	1.67 ± 0.93	0.61 ± 0.14	1.14 ± 0.47
SUTL2969/16	60.0 ± 9.2	47.4 ± 9.1	53.7 ± 6.5	0.888 ± 0.203	1.296 ± 0.313	1.092 ± 0.187	1.73 ± 0.14	0.77 ± 0.11	1.25 ± 0.09
SUTL2969/17	27.3 ± 9.1	1.3 ± 9.1	14.3 ± 6.4	1.123 ± 0.503	11.83 ± 85.52	6.48 ± 42.76	0.81 ± 0.14	0.39 ± 0.19	0.60 ± 0.12
SUTL2969/18	51.6 ± 9.3	4.8 ± 9.1	28.2 ± 6.5	0.780 ± 0.227	5.83 ± 11.08	3.303 ± 5.539	0.26 ± 0.10	1.51 ± 0.39	0.88 ± 0.20
SUTL2969/19	27.5 ± 9.6	47.4 ± 9.6	37.5 ± 6.8	0.763 ± 0.439	1.128 ± 0.303	0.946 ± 0.267	0.65 ± 0.08	0.17 ± 0.08	0.41 ± 0.06
SUTL2969/20	72.6 ± 9.6	31.1 ± 8.9	51.8 ± 6.6	0.751 ± 0.163	1.257 ± 0.457	1.004 ± 0.243	0.38 ± 0.08	0.06 ± 0.18	0.22 ± 0.10
SUTL2969/21	32.3 ± 9.5	-3.6 ± 9.2	14.4 ± 6.6	1.968 ± 0.646	-10.00 ± 25.91	-4.02 ± 12.96	-0.02 ± 0.07	0.71 ± 0.15	0.34 ± 0.09
SUTL2970A	34.0 ± 9.2	34.4 ± 9.2	34.2 ± 6.5	0.377 ± 0.282	1.787 ± 0.554	1.082 ± 0.311	0.76 ± 0.19	0.34 ± 0.09	0.55 ± 0.10
SUTL2970B	31.1 ± 8.4	9.4 ± 9.0	20.3 ± 6.2	1.534 ± 0.508	0.044 ± 0.983	0.789 ± 0.553	0.27 ± 0.16	0.56 ± 0.16	0.41 ± 0.11
SUTL2970C	59.6 ± 9.4	81.7 ± 10.5	70.6 ± 7.1	1.137 ± 0.240	1.666 ± 0.251	1.402 ± 0.174	-0.09 ± 0.11	0.04 ± 0.03	-0.02 ± 0.06

Table A.4: Results of TL profiling of polymineral fractions, for each aliquot and the mean values. Showing sensitivity (from D1 response), sensitivity change (ratio of D3 to D1) and dose estimates (from natural and D2 responses).

Sample	Sensitivity c Gy^{-1}			Sensitivity change			Dose estimate Gy		
	Al 1	Al 2	Mean	Al 1	Al 2	Mean	Al 1	Al 2	Mean
SUTL2969/1	5318 ± 33	4102 ± 29	4710 ± 22	1.094 ± 0.010	1.069 ± 0.011	1.081 ± 0.007	8.211 ± 0.021	7.535 ± 0.023	7.873 ± 0.015
SUTL2969/2	14154 ± 55	14361 ± 55	14257 ± 39	1.070 ± 0.006	0.933 ± 0.005	1.001 ± 0.004	7.655 ± 0.012	7.868 ± 0.013	7.762 ± 0.009
SUTL2969/3	11146 ± 48	22227 ± 68	16687 ± 42	0.927 ± 0.006	1.019 ± 0.004	0.973 ± 0.004	7.286 ± 0.014	7.583 ± 0.010	7.435 ± 0.008
SUTL2969/4	10673 ± 47	15390 ± 57	13032 ± 37	1.068 ± 0.007	1.259 ± 0.006	1.164 ± 0.005	6.593 ± 0.012	6.854 ± 0.011	6.724 ± 0.008
SUTL2969/5	10501 ± 47	10333 ± 47	10417 ± 33	0.999 ± 0.006	0.981 ± 0.006	0.990 ± 0.004	7.058 ± 0.014	7.138 ± 0.014	7.098 ± 0.010
SUTL2969/6	13926 ± 54	11312 ± 49	12619 ± 36	1.057 ± 0.006	1.061 ± 0.006	1.059 ± 0.004	6.878 ± 0.011	7.616 ± 0.013	7.247 ± 0.009
SUTL2969/7	16675 ± 59	15200 ± 56	15938 ± 41	1.012 ± 0.005	0.965 ± 0.005	0.988 ± 0.004	6.678 ± 0.010	7.289 ± 0.012	6.983 ± 0.008
SUTL2969/8	11031 ± 48	17169 ± 60	14100 ± 38	1.028 ± 0.006	1.102 ± 0.005	1.065 ± 0.004	5.306 ± 0.010	5.077 ± 0.008	5.191 ± 0.007
SUTL2969/9	6643 ± 37	7470 ± 40	7056 ± 27	1.064 ± 0.008	1.041 ± 0.008	1.052 ± 0.006	7.04 ± 0.017	6.667 ± 0.015	6.853 ± 0.011
SUTL2969/10	18230 ± 62	22421 ± 69	20326 ± 46	1.102 ± 0.005	1.040 ± 0.004	1.071 ± 0.003	5.451 ± 0.008	5.753 ± 0.008	5.602 ± 0.006
SUTL2969/11	8015 ± 41	8165 ± 41	8090 ± 29	1.004 ± 0.007	1.083 ± 0.008	1.043 ± 0.005	5.259 ± 0.012	5.122 ± 0.012	5.191 ± 0.009
SUTL2969/12	13816 ± 54	16485 ± 59	15151 ± 40	1.085 ± 0.006	1.079 ± 0.005	1.082 ± 0.004	4.550 ± 0.008	4.814 ± 0.008	4.682 ± 0.006
SUTL2969/13	8879 ± 43	8335 ± 42	8607 ± 30	1.117 ± 0.007	1.126 ± 0.008	1.122 ± 0.005	3.840 ± 0.009	4.174 ± 0.010	4.007 ± 0.007
SUTL2969/14	7336 ± 39	8657 ± 43	7997 ± 29	1.052 ± 0.008	1.081 ± 0.007	1.066 ± 0.005	4.394 ± 0.011	4.237 ± 0.010	4.315 ± 0.007
SUTL2969/15	5131 ± 33	4968 ± 32	5050 ± 23	1.001 ± 0.009	1.056 ± 0.010	1.029 ± 0.007	3.641 ± 0.012	3.827 ± 0.012	3.734 ± 0.008
SUTL2969/16	11969 ± 50	11986 ± 50	11977 ± 35	1.077 ± 0.006	1.071 ± 0.006	1.074 ± 0.004	3.150 ± 0.007	3.075 ± 0.007	3.113 ± 0.005
SUTL2969/17	8380 ± 42	9837 ± 45	9109 ± 31	1.115 ± 0.008	1.169 ± 0.007	1.142 ± 0.005	2.792 ± 0.007	2.776 ± 0.007	2.784 ± 0.005
SUTL2969/18	9559 ± 45	8013 ± 41	8786 ± 30	1.190 ± 0.008	1.224 ± 0.008	1.207 ± 0.006	2.424 ± 0.006	2.368 ± 0.007	2.396 ± 0.005
SUTL2969/19	13475 ± 53	11313 ± 49	12394 ± 36	1.185 ± 0.006	1.098 ± 0.007	1.141 ± 0.005	2.039 ± 0.005	2.205 ± 0.005	2.122 ± 0.004
SUTL2969/20	14753 ± 56	8836 ± 43	11795 ± 35	1.087 ± 0.006	1.132 ± 0.008	1.109 ± 0.005	1.961 ± 0.004	1.685 ± 0.005	1.823 ± 0.003
SUTL2969/21	8665 ± 43	9320 ± 44	8993 ± 31	1.114 ± 0.008	1.145 ± 0.007	1.129 ± 0.005	1.120 ± 0.004	1.211 ± 0.004	1.165 ± 0.003
SUTL2970A	6847 ± 38	16503 ± 59	11675 ± 35	1.136 ± 0.009	1.042 ± 0.005	1.089 ± 0.005	7.010 ± 0.016	8.064 ± 0.012	7.537 ± 0.010
SUTL2970B	11496 ± 49	13533 ± 53	12514 ± 36	1.021 ± 0.006	1.088 ± 0.006	1.054 ± 0.004	7.200 ± 0.013	6.627 ± 0.011	6.914 ± 0.008
SUTL2970C	15846 ± 58	14602 ± 55	15224 ± 40	0.950 ± 0.005	1.040 ± 0.006	0.995 ± 0.004	2.419 ± 0.005	2.656 ± 0.006	2.537 ± 0.004

Appendix B: SAR dose responses and dose distributions

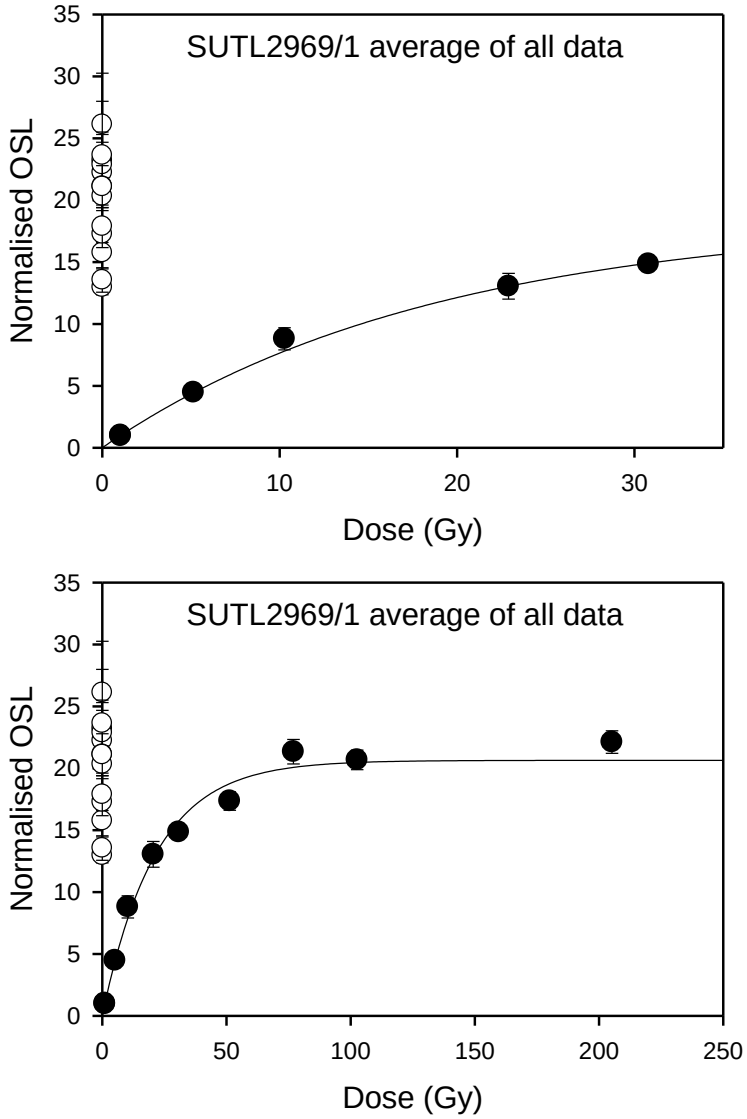

Figure B.1: Dose response curves for SUTL2969/1, showing normalised OSL for the natural signals. Initial dose range (top) and extended dose range (bottom).

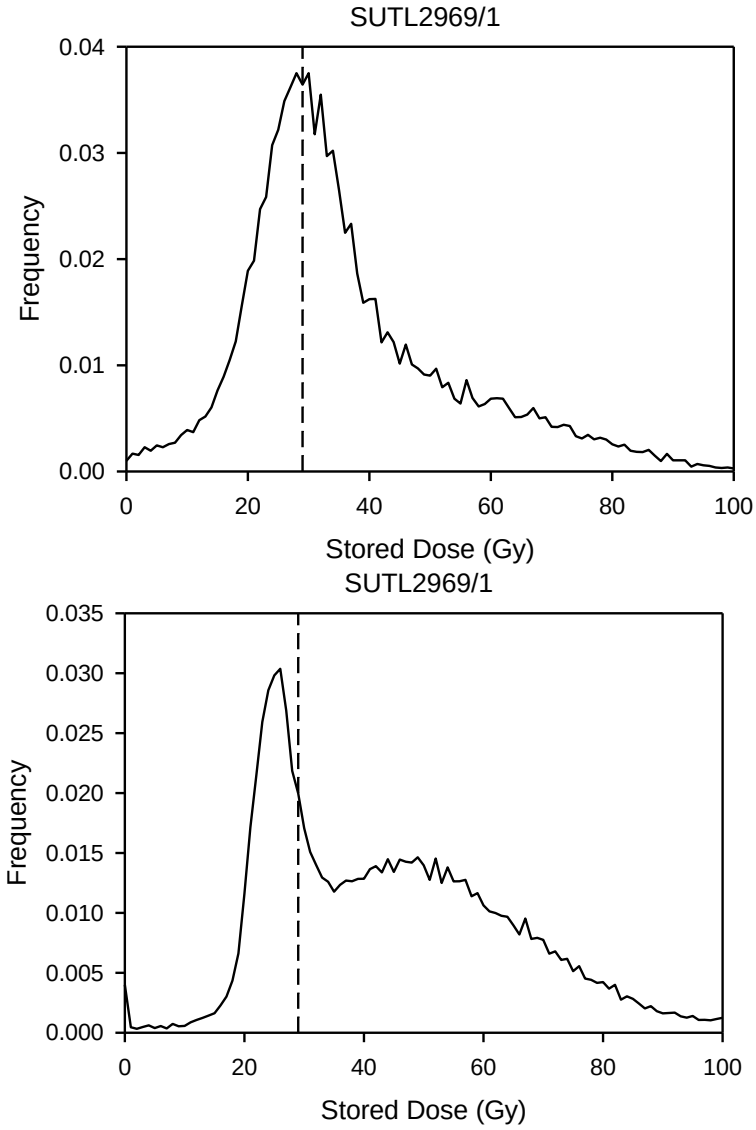

Figure B.2: PDF plot for SUTL2969/1; top showing initial measurements for four unsaturated aliquots that satisfy SAR quality criteria, bottom following extended dose measurements with nine unsaturated aliquots that satisfy SAR quality criteria. The weighted mean is indicated.

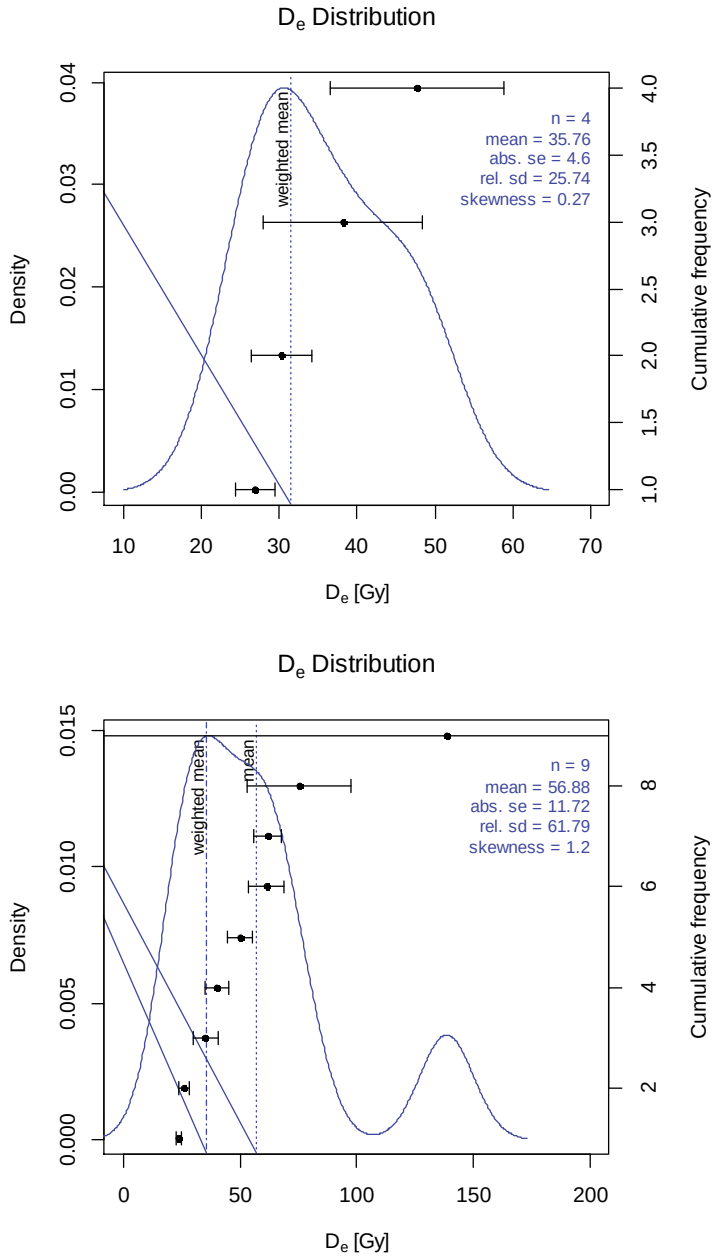

Figure B.3: KDE plots for SUTL2969/1, top for initial measurement with four unsaturated aliquots that satisfy SAR quality criteria, bottom for the extended dose response measurement with nine unsaturated aliquots.

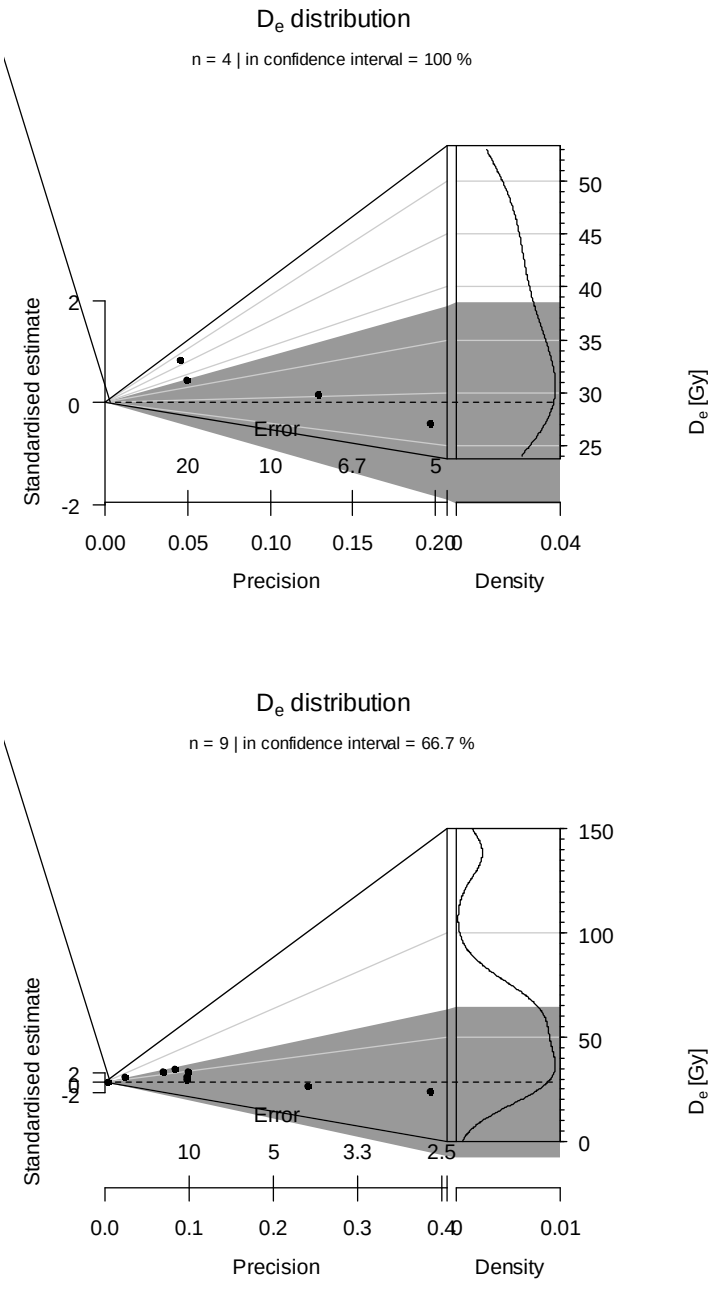

Figure B.4: Abanico plots for SUTL2969/1, top for initial analysis with four unsaturated aliquots that satisfy SAR quality criteria, bottom for the extended dose analysis with nine unsaturated aliquots, The weighted mean is indicated.

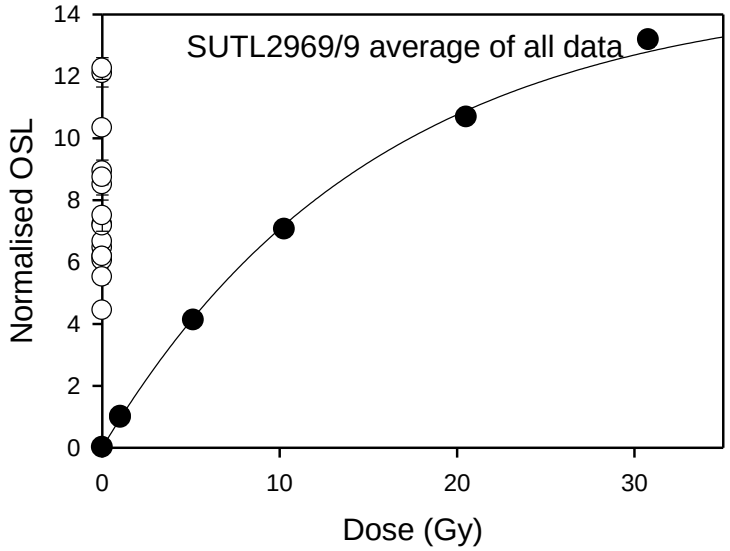

Figure B.5: Dose response curve for SUTL2969/9, showing normalised OSL for the natural signals.

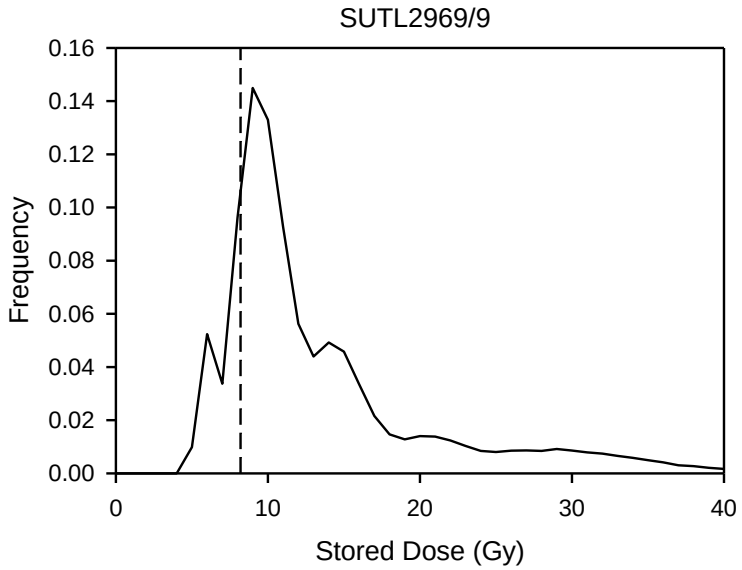

Figure B.6: PDF plot for SUTL2969/9. The weighted mean is indicated.

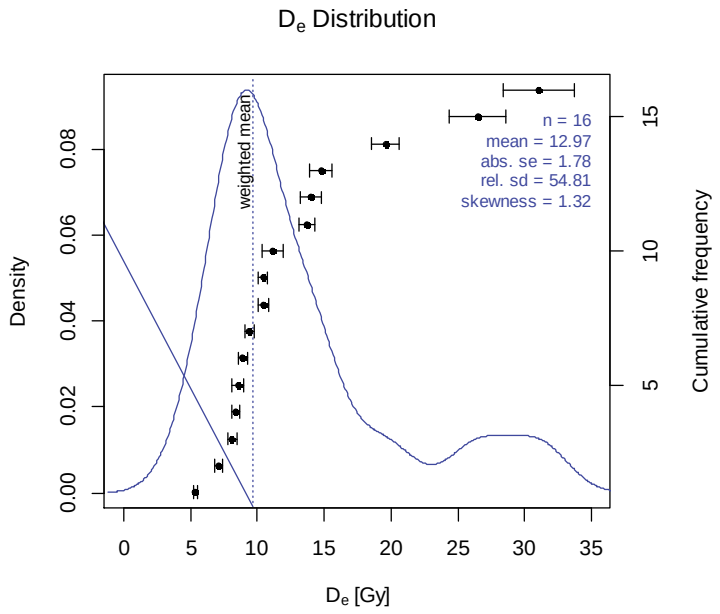

Figure B.7: KDE plot for SUTL2969/9

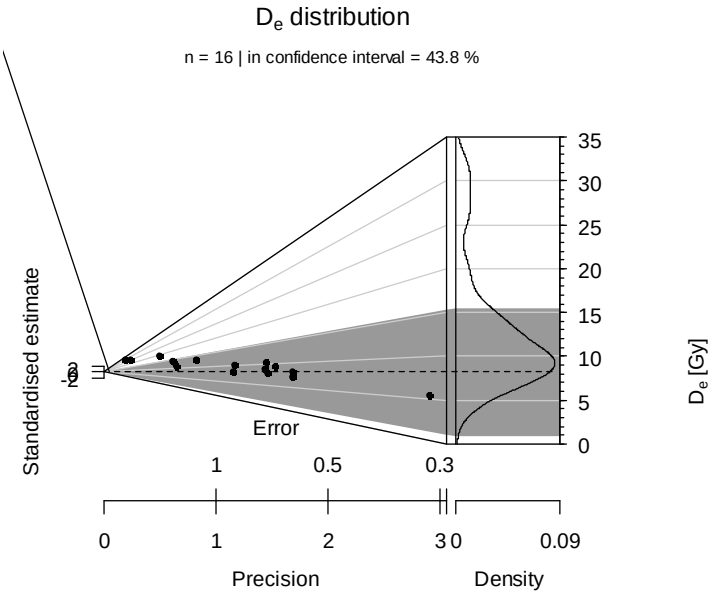

Figure B.8: Abanico plot for SUTL2969/9

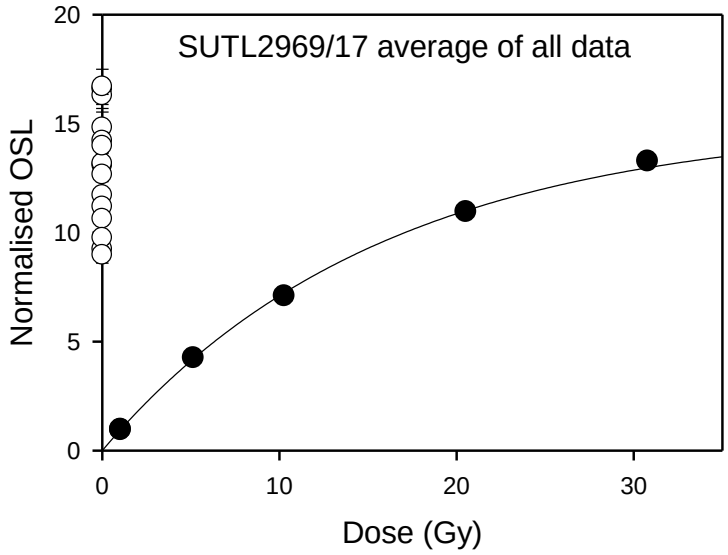

Figure B.9: Dose response curve for SUTL2969/17, showing normalised OSL for the natural signals.

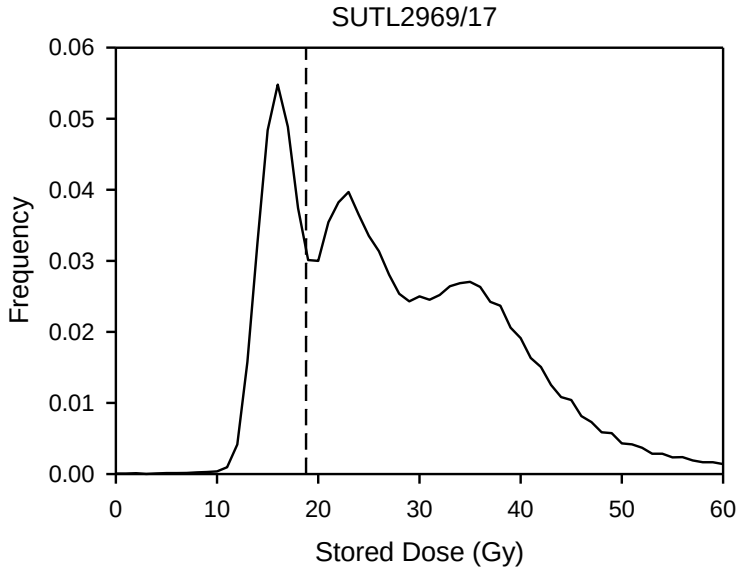

Figure B.10: PDF plot for SUTL2969/17. The weighted mean is indicated.

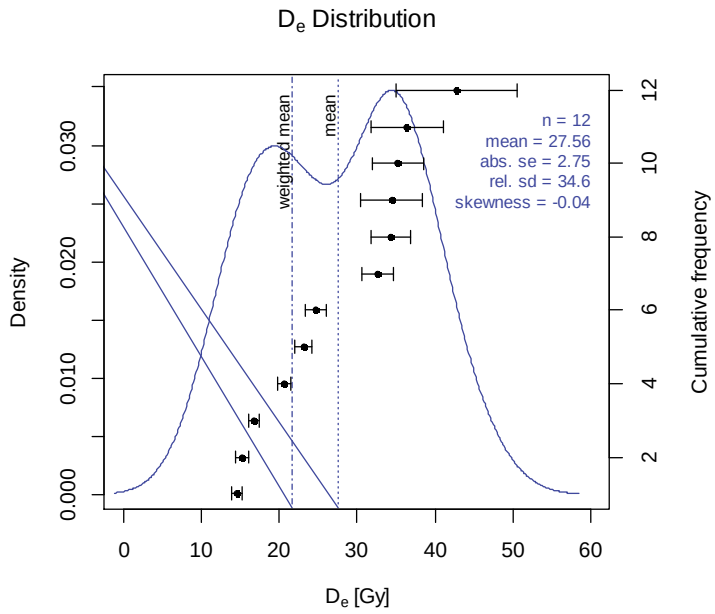

Figure B.11: KDE plot for SUTL2969/17

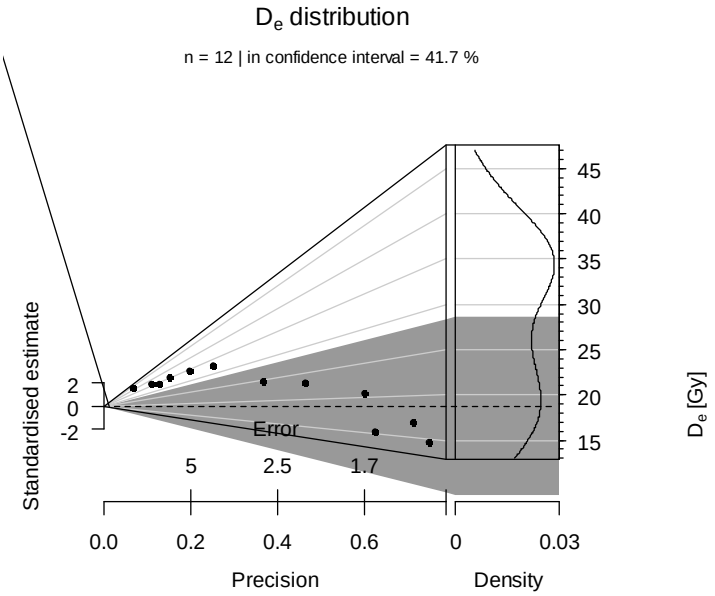

Figure B.12: Abanico plot for SUTL2969/17